

Identification of *PPAP2B* as a Novel Recurrent Translocation Partner Gene of *HMGA2* in Lipomas

Laurence Bianchini,^{1,2*} Loïc Birtwisle,^{1,2} Esma Saâda,^{1,2,3} Audrey Bazin,^{1,2} Elodie Long,⁴ Jean-François Roussel,⁵ Jean-François Michiels,⁶ Fabien Forest,⁷ Christian Dani,⁸ Ola Myklebost,⁹ Isabelle Birtwisle-Peyrottes,¹⁰ and Florence Pedeutour^{1,2}

¹Laboratory of Solid Tumors Genetics, Nice University Hospital, Nice, France

²Institute for Research on Cancer and Aging of Nice (IRCAN), CNRS UMR 7284/INSERM UI081, University of Nice-Sophia Antipolis, Nice, France

³Medical Oncology Department, Centre Antoine-Lacassagne, Nice, France

⁴Laboratory of Clinical and Experimental Pathology and Human Tissue Biobank/CRB INSERM, Nice University Hospital, Nice, France

⁵Department of Pathology, Princess Grace Hospital, Monaco, Monaco

⁶Central Laboratory of Pathology, Nice University Hospital, Nice, France

⁷Department of Pathology and Tumor BioBank (CRB-TK 42), Saint Etienne University Hospital, Saint-Etienne, France

⁸Institute of Biology Valrose, UMR7277 CNRS/UMRI091 INSERM/University of Nice-Sophia Antipolis, Nice, France

⁹Department of Tumor Biology, Institute for Cancer Research, The Norwegian Radium Hospital, Oslo University Hospital, Oslo, Norway

¹⁰Laboratory of Cytology and Pathology, Centre Antoine-Lacassagne, Nice, France

Most lipomas are characterized by translocations involving the *HMGA2* gene in 12q14.3. These rearrangements lead to the fusion of *HMGA2* with an ectopic sequence from the translocation chromosome partner. Only five fusion partners of *HMGA2* have been identified in lipomas so far. The identification of novel fusion partners of *HMGA2* is important not only for diagnosis in soft tissue tumors but also because these genes might have an oncogenic role in other tumors. We observed that t(1;12)(p32;q14) was the second most frequent translocation in our series of lipomas after t(3;12)(q28;q14.3). We detected overexpression of *HMGA2* mRNA and protein in all t(1;12)(p32;q14) lipomas. We used a fluorescence in situ hybridization-based positional cloning strategy to characterize the 1p32 breakpoint. In 11 cases, we identified *PPAP2B*, a member of the lipid phosphate phosphatases family as the 1p32 target gene. Reverse transcription-polymerase chain reaction analysis followed by nucleotide sequencing of the fusion transcript indicated that *HMGA2* 3' untranslated region (3'UTR) fused with exon 6 of *PPAP2B* in one case. In other t(1;12) cases, the breakpoint was extragenic, located in the 3' region flanking *PPAP2B* 3'UTR. Moreover, in one case showing a t(1;6)(p32;p21) we observed a rearrangement of *PPAP2B* and *HMGA1*, which suggests that *HMGA1* might also be a fusion partner for *PPAP2B*. Our results also revealed that adipocytic differentiation of human mesenchymal stem cells derived from adipose tissue was associated with a significant decrease in *PPAP2B* mRNA expression suggesting that *PPAP2B* might play a role in adipogenesis. © 2013 Wiley Periodicals, Inc.

INTRODUCTION

Lipomas are the most frequent mesenchymal tumors in humans. These benign adipose tumors occur mainly in the fourth to sixth decades. Most of them appear as small, well-circumscribed painless subcutaneous masses located in the upper back, neck, shoulders, arms or thighs. Occasionally they can be deeply situated, infiltrating the surrounding tissues or comprise a few atypical cells that make them difficult to distinguish from liposarcomas. Cytogenetic and molecular analyses are useful as complementary tools for differential diagnosis. Indeed, approximately two-thirds of lipomas are characterized by chromosomal aberrations (Mandahl et al., 1994; Fletcher et al., 2002). Among these lipomas exhibiting an abnormal karyotype, three major subgroups have been

described: structural rearrangements of the 12q14 region are detected in two-thirds of the cases, followed by anomalies of the 13q12–22 region (15%) and rearrangements of the 6p21 region (5%). Rearrangements of the 12q14 region include

Additional Supporting Information may be found in the online version of this article.

Supported by: Association pour la Recherche sur le Cancer, Grant number: ARC 4008; Institut National du Cancer (projet libre "GENOSTT"); Cancéropôle Provence Alpes Côte d'Azur; Conseil Régional Provence Alpes Côte d'Azur.

*Correspondence to: Laurence Bianchini, Laboratoire de Génétique des Tumeurs Solides, Faculté de Médecine, 28 avenue de Valombrose, 06107 Nice cedex 02, France.

E-mail: laurence.bianchini@unice.fr

Received 25 November 2012; Accepted 6 February 2013

DOI 10.1002/gcc.22055

Published online in Wiley Online Library (wileyonlinelibrary.com).

translocations involving a large variety of chromosomal regions, inversions, insertions or deletions (Nishio, 2011; Mitelman et al., 2012). These rearrangements frequently result in fusion of the *HMGA2* (12q14.3) gene with several partner genes (Ashar et al., 1995; Schoenmakers et al., 1995; Fedele et al., 1998; Fletcher et al., 2002; Italiano et al., 2008b). Breakpoints have been reported to occur preferentially in the large third intron of *HMGA2* (Ashar et al., 1995) resulting either in the expression of a truncated protein lacking the acidic COOH-terminal region and the 3' untranslated region (3'UTR) or in the expression of a chimeric protein fusing the *HMGA2* AT-hooks domains to an ectopic sequence from the fusion partner (Ashar et al., 1995; Petit et al., 1996; Bartuma et al., 2007). Strikingly, although more than 40 chromosome bands have been described in rearrangements involving the 12q13-15 region in lipomas (Bartuma et al., 2007), only five genes have been identified as fusing with *HMGA2* so far: *LPP* (3q28), *CXCR7* (2q37), *EBF* (5q33), *LHFP* (13q12) and *NFIB* (9p22) (Petit et al., 1996, 1999; Broberg et al., 2002; Nilsson et al., 2005, 2006; Hatano et al., 2008; Italiano et al., 2008b). The most frequent fusion is *HMGA2-LPP*, detected in 20% of lipomas, which results in the fusion of the three AT-hooks of *HMGA2* to the LIM domains of *LPP*. *LPP*, for "Lipoma Preferred Partner," first identified in lipomas (Ashar et al., 1995; Schoenmakers et al., 1995) then in pulmonary chondroid hamartomas (Rogalla et al., 1998) as well as in chondroma (Dahlén et al., 2003), was subsequently found to be overexpressed in malignant tumors such as lung carcinomas (Choi et al., 2007) and sarcomas (Hussenet et al., 2006). Similarly, *NFIB* a gene that fused with *HMGA2* in pleomorphic adenomas of salivary glands (Geurts et al., 1998) and in t(9;12) lipomas (Nilsson et al., 2005; Italiano et al., 2008b; Pierron et al., 2009) was further shown to be overexpressed and oncogenic in small cell lung cancer (Dooley et al., 2011); amplified in a mouse model of prostate cancer (Zhou et al., 2006) and in patients with triple negative breast cancer (Han et al., 2008). Characterization of new fusion partners of *HMGA2* is therefore potentially useful for advances in molecular diagnosis of adipose tumors and for identification of candidate genes in malignant tumors. Here, we describe the identification of a novel recurrent translocation partner gene of *HMGA2* in lipomas showing t(1;12)(p32;q14) translocations.

MATERIALS AND METHODS

Cytogenetic, Histological, and Clinical Data

Sixteen cases were selected from our series of 418 lipomas analyzed between 1993 and 2012 at the Laboratory of Solid Tumor Genetics (Nice, France) because their RHG-banded karyotypes obtained from short term primary cell cultures showed the presence of a rearrangement of the 1p32 region and enough biological material was available for further fluorescence in situ hybridization (FISH) or expression analysis. These 1p32 rearrangements were either t(1;12)(p32;q14-15) (cases 1–15), sometimes in association with additional anomalies or t(1;6)(p32;p21) (case 16) (Table 1). The clinico-pathologic characteristics of the 16 cases are listed in Table 1. Histologically, all cases were ordinary lipomas. Atypias or lipoblasts were not detected. With the exception of one case showing intramuscular infiltration (case 5), and one case located in the caecal wall (case 12), no clinical or histological peculiar features were noted. All lipomas measured less than 15 cm in their largest axis (average size: 8 cm). In all cases, the diagnosis of lipoma was established according to the World Health Organization Classification of Tumors (Fletcher et al., 2002).

FISH Analyses

The FISH probes used in this study are listed in Table 2. We used sets of BAC probes located in the 12q14.3, 6p21, and 1p32.1-1p32.3 regions. The BAC clones from the Roswell Park Cancer Institute library were selected according to their location on the University of California Santa Cruz database (hg19, Feb. 2009, GRCh37 Genome 5 Reference Consortium Human Reference 37; <http://www.genome.ucsc.edu>) purchased from the Children's Hospital Oakland Research Institute (CHORI, <http://bacpaschori.org/>) or from Invitrogen (Carlsbad, CA) and prepared as probes for FISH analysis according to standard procedures. For each probe, the chromosomal location was verified by FISH on normal metaphases cells from peripheral blood lymphocytes. Microscopic analysis was performed using a DM6000B microscope (Leica Microsystems, Wetzlar, Germany). FISH images were processed using the ISIS software (Metasystems, Altussheim, Germany).

RNA Isolation and Reverse Transcription-Polymerase Chain Reaction

Twenty 5- μ M thick tissue sections from formalin-fixed paraffin embedded case 10 were

TABLE 1. Clinicopathologic and Cytogenetic Characteristics of 16 Cases of Lipomas with Ip32 Rearrangements

Case	Laboratory identification	Sex/age (year)	Size (cm)/weight (g)	Location	Partial RHG-banded karyotype	Breakpoint in <i>HMGA2</i> region ^a
1	93T639	M	ND	ND	t(1;12)(p32;q14)	+
2	09T089	M/56	14.5 × 6	Right calf	t(1;12)(p32;q14),del(13)(q14q31)	+
3	10T355	F/48	11 × 6 × 2/56	Right shoulder	t(1;12)(p32;q14)	+
4	10T777	M/61	14 × 9.5 × 3.5/134	Left hip	t(1;12)(p32;q14)	+
5	11T350	M/60	4.5 × 3.5 × 2/16	Right cheek	t(1;12)(p32;q14)	+
6	11T369^b	M/17	4 × 3.5 × 2.5/10	Right arm	Complex rearrangement involving 1p;7q;12q	+
7	11T874	F/38	9 × 6.5 × 3.5/61	Right shoulder	t(1;12)(p32;q14)	+
8	11T1233	M/37	11.7 (largest axis)	Left buttock	t(1;12)(p32;q14),t(1;20)(q32;p13)	+
9	05T312	M/51	10 × 6 × 6.5/94	Left buttock	t(1;12)(p32;q14),t(1;12)(q13;p13)	+
10	10T706	M/55	5.5 × 4.5 × 2.5/20	Right chest wall	t(1;12)(p32;q14)	+
11	09T699	F/64	6.5 × 4.1 × 1.5/16	Left forearm	t(1;12)(p32;q14), del(1)(p32), t(2;11)(q21;p15)	+
12	94T685^c	F/57	4 × 2.5	Caecal wall	t(1;12)(p32;q14)	+
13	10T034	F/36	10 × 7 × 4/80	Paravertebral	inv(1)(p32q11),t(1;12)(q11;q14), t(17;18)(q11;q23)	Deletion
14	11T124	F/56	4.2 × 4.2 × 2	Right axilla	t(1;12;19)(p32;q13;q11)	–
15	07T614	M/43	6 × 3/38	Right scapula	t(1;12)(p32;q14)	–
16	12T893	M/54	5 × 3.5 × 1	Back	t(1;6)(p32;p21)	ND ^d

F, female; M, male; ND, not done.

^aBased on FISH analysis using RP11-30111 and RP11-118B13 probes.

^bContext of multiple lipomas.

^cPublished in Bianchini et al. (2011).

^dBreakpoint in *HMGA1* region.

TABLE 2. Description of the FISH Probes Used for the Characterization of the Ip32.2; 6p21 and 12q14.3 Regions in 10 Cases of Lipomas with t(1;12)(p32.2;q14.3) and One Case of Lipoma with t(1;6)(p32.2;p21)

Probe identification	Locus/chromosomal location/position ^a
Ip32 probes	
RP11-63G10	<i>JUN1</i> /1p32.1/59,179,090–59,321,753
RP11-20I22	<i>PPAP2B</i> 5' region/1p32.2/57,050,331–57,210,976
CTD-2362O17	<i>PPAP2B</i> /1p32.2/56,944,572–57,040,951
RP11-100M11	<i>PPAP2B</i> /1p32.2/56,926,040–57,085,832
RP11-213P13	<i>PPAP2B</i> /1p32.2/56,881,261–57,050,325
RP11-1089D11	<i>PPAP2B</i> /1p32.2/56,811,847–57,012,937
RP11-97I16	<i>PPAP2B</i> 3' region/1p32.2/56,711,452–56,866,789
RP11-606D16	<i>PPAP2B</i> 3' region/1p32.2/56,695,211–56,856,280
RP11-485A11	<i>PPAP2B</i> 3' region/1p32.3/55,708,546–55,908,106
RP11-154H10	<i>PPAP2B</i> 3' region/1p32.3/55,014,287–55,187,057
CTD-2171C24	<i>PPAP2B</i> 3' region/1p32.3/50,512,939–50,651,490
RP11-49M17	<i>ACOT11</i> /1p32.3/55,032,301–55,206,162
6p21 probes	
CTD-2527O17	<i>HMGA1</i> 3' region/6p21.31/34,227,823–34,405,143
CTD-2342D14	<i>HMGA1</i> 3' region/6p21.31/34,250,856–34,406,390
RP11-754H10	<i>HMGA1</i> 5' region/6p21.31/33,852,410–34,029,251
RP11-661K21	<i>HMGA1</i> 5' region/6p21.31/33,841,325–34,029,245
12q14 probes	
RP11-118B13	<i>HMGA2</i> (3' UTR)/12q14.3/66,358,701–66,502,988
CTD-2240K5	<i>HMGA2</i> (exons 4, 5; 3' UTR)/12q14.3/66,325,027–66,457,979
RP11-427K2	<i>HMGA2</i> (exons 4, 5; 3' UTR)/12q14.3/66,323,478–66,481,711
CTC-78219	<i>HMGA2</i> (exon 4)/12q14.3/66,235,316–66,355,707
RP11-23C9	<i>HMGA2</i> (5' UTR; exons 1, 2, 3)/12q14.3/66,093,846–66,246,663
RP11-30I11	<i>HMGA2</i> 5' region/12q14.3/65,892,238–66,063,441

^ahg19, Feb. 2009, GRCh37 Genome 5 Reference Consortium Human Reference 37; <http://www.genome.ucsc.edu>.

deparaffinized in xylene and dehydrated in 100% ethanol. Following proteinase K digestion, total RNA was extracted using TRIzol reagent (Invitrogen) according to the manufacturer's instructions. cDNA was synthesized from RNA and amplified (SuperScript One-Step RT-PCR kit, Invitrogen) using the following primers: forward primer HMGA2-2F: 5'-AACCGGTGAGCCC TCTCCTA-3'; reverse primer PPAP2B-6R1420 5'-GAGCGTCGTCTTAGTCTTGAAG-3'. The reverse transcription-polymerase chain reaction (RT-PCR) were carried out as follows: 30 min at 55°C, 94°C for 5 min; 94°C for 30 sec, 58°C for 30 sec, 72°C for 30 sec, 72°C for 7 min; 45 cycles. β -actin-specific primers (ACTIN-F1: 5'-ACCAAC TGGGACGACATGGAGAAA-3' and ACTIN-R: 5'-GGGATAGCACAGCCTGGATAGCA-3') were used for quality control RT-PCR (amplification of a 196-bp sequence). Aliquots from RT-PCR products were visualized in a 1% agarose gel stained with ethidium bromide after electrophoretic migration. The bands of interest were extracted from the gel, purified using an ultrafree DNA column (Millipore, Billerica, MA), cloned into pCR4-TOPO vector and transformed into One Shot TOP10 *Escherichia coli* competent cells (Topo Cloning Kit for Sequencing, Invitrogen). The clones were screened by PCR using M13 forward primer (5'-GTAAACGACGGCCAG-3') and M13 reverse primer (5'-CAGGAAACAGC TATGAC-3') and the clones of interest were sequenced by using the Sequenase kit version 2.0 (USB, Cleveland, OH).

Quantitative RT-PCR Analysis (qRT-PCR)

Total RNA was extracted from lipomas (six cases), normal subcutaneous adipose tissue (NSAT), and human multipotent adipose-derived stem (hMADS) cells using the RNeasy lipid tissue mini Kit (Qiagen, Hilden, Germany). The RNA samples were treated using the DNA-free kit (Applied Biosystems). The quality of the isolated RNA was determined using the 2100 BioAnalyser (Agilent Technologies, Santa Clara, CA) using the RNA 6000 Nano Kit (Agilent Technologies). One microgram of total RNA was reverse-transcribed into cDNA using the High Capacity cDNA Reverse Transcription Kit (Applied Biosystems). *RPLP0* and *TBP* were used as endogenous controls for normalization of experiments in lipomas and hMADS cells, respectively (Gabrielsson et al., 2005). QRT-PCR was performed using the following TaqMan gene

expression assays (Applied Biosystems): Hs00171569_m1 (*HMGA2*, exons 1–2), Hs00971724_m1 (*HMGA2*, exons 3–4), Hs00971725_m1 (*HMGA2*, exons 4–5), Hs00170359_m1 (*PPAP2B*, exons 1–2), Hs01009653_m1 (*PPAP2B*, exons 4–5), Hs99999902_m1 (*RPLP0*), Hs00427620_m1 (*TBP*). The reaction mix consisted of 10 μ l of TaqMan universal master mix 2 \times , 1 μ l of TaqMan gene expression assay and 5 μ l containing 5 ng of cDNA in a final volume of 20 μ l.

The PCR conditions were as described previously (Italiano et al., 2008a). The comparative threshold cycle method was used to achieve relative quantification of gene expression (Italiano et al., 2008a). Each q-PCR experiment was performed three times in duplicate using the ABI PRISM 7500 Detection System (FAM dyes; Applied Biosystems) according to the manufacturer's instructions.

Immunohistochemistry

Immunohistochemistry (IHC) studies were performed on 4- μ m thick sections of formalin-fixed paraffin-embedded tissues from 15 lipomas using a BenchMark XT immunostainer (Ventana, Tucson, AZ) and a rabbit polyclonal antihuman HMGA2-P1 antibody (Biocheck, Foster city, CA) at a dilution of 1:500 as described previously (Bianchini et al., 2011). Well-differentiated liposarcoma (WDLPS) and adult normal subcutaneous adipose tissue samples were used as positive and negative controls, respectively. The slides were examined (I.B-P) in a blinded manner.

hMADS Cell Culture and Adipocyte-Differentiation

hMADS cells were isolated from white adipose tissue of young donors as described previously (Rodriguez et al., 2005). Self-renewal properties and ability of these cells to differentiate into adipocytes have been extensively described (Zaragosi et al., 2006). hMADS cells were grown in Dulbecco's modified Eagle's medium (DMEM) supplemented with 10% fetal calf serum, 2.5 ng/ml human fibroblast growth factor (hFGF)-2, 60 μ g/ml penicillin and 50 μ g/ml streptomycin. hFGF-2 was removed when cells reached confluence. Adipocyte differentiation was performed as follows: on day 0, confluent hMADS cells were cultured in differentiation medium: DMEM low glucose/Ham's F12 supplemented with the following adipogenic cocktail: transferrin (10 μ g/ml), insulin (5 μ g/ml),

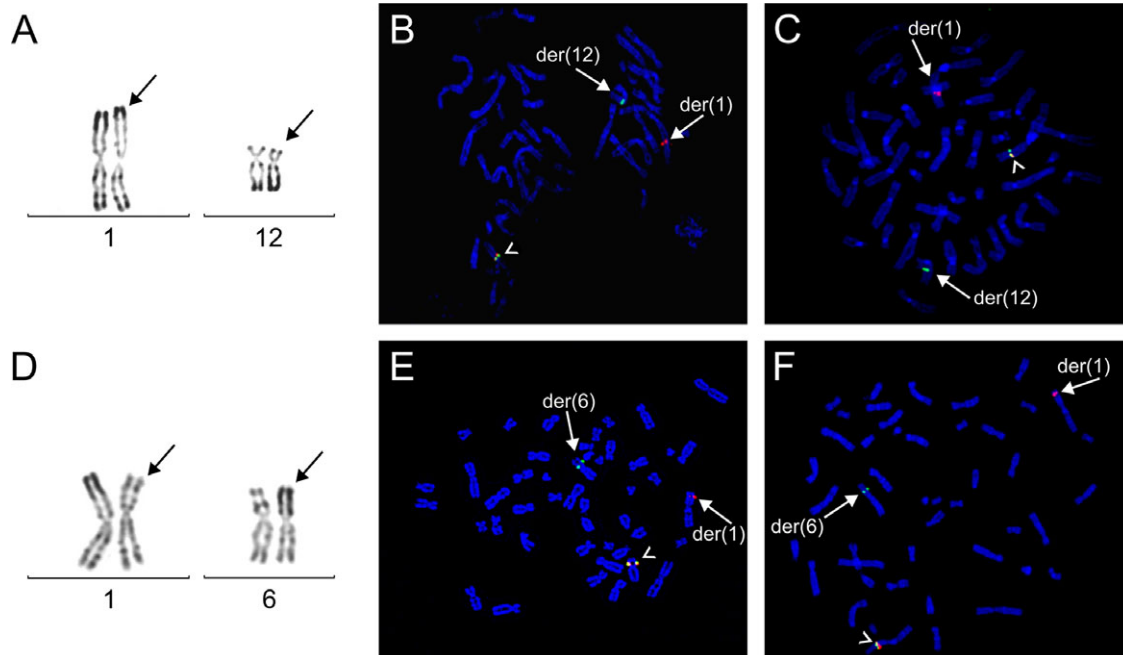


Figure 1. Chromosomal region 1p32 anomalies and genic rearrangements in lipoma cases 3 (A–C) and 16 (D–F). A and D: Partial RHG-banded karyotypes showing $t(1;12)(p32;q14)$ (A) and $t(1;6)(p32;p21)$ (D). Arrows indicate the der(1), der(12) (A) and der(6) (D) resulting from the translocations. B: The dual-color break-apart FISH probes set RP11-30I11 (*HMGA2* 5' region; green signal) and RP11-118B13 (*HMGA2* 3' region; red signal) demonstrates rearrangement of *HMGA2* region. The arrows indicate der(1) (red signal) and der(12) (green signal), respectively. Overlapped green/red signals correspond to the normal allele (arrowhead) on 12q14.3. C and F: The dual-color break-apart FISH probes set RP11-485A11 (telomeric to the *PPAP2B* 3'UTR region; green signal) and

RP11-20I22 (flanking the *PPAP2B* 5'UTR region; red signal) demonstrates rearrangement of *PPAP2B* region. The arrows indicate der(1) (red signal), der(12) (green signal) (C) and der(6) (F), respectively. Overlapped green/red signals correspond to the normal allele (arrowhead) on 1p32.2. E: The dual-color break-apart FISH probes set RP11-754H10/RP11-661K21 (flanking *HMGA1* 5' region; red signal) and CTD-2527O17/CTD-2342D14 (flanking *HMGA1* 3' region; green signal) demonstrates rearrangement of *HMGA1* region. Arrows indicate der(1) (red signal) and der(6) (green signal), respectively. Overlapped green/red signals correspond to the normal allele (arrowhead) on 6p21. [Color figure can be viewed in the online issue, which is available at wileyonlinelibrary.com.]

triiodothyronine (0.2 nM), dexamethasone (1 μ M), isobutyl-methylxanthine (100 μ M) and rosiglitazone (1 μ M). Three days later (day 3), the medium was changed: dexamethasone and isobutyl-methylxanthine were omitted.

RESULTS

FISH Positional Cloning Data: Identification of *HMGA2* in 12q14.3, *HMGA1* in 6p21 and *PPAP2B* in 1p32 as Candidate Fusion Genes

We used a FISH-based positional cloning strategy to define the chromosomal breakpoints in 15 cases of lipomas showing simple balanced or complex $t(1;12)$ (cases 1–15) (illustrated for case 3, Fig. 1A) and the one case showing a $t(1;6)$ (case 16) (Fig. 1D). In cases 1–12, we observed breakpoints located within the interval containing *HMGA2* framed by probes RP11-30I11 and RP11-118B13 (chr12: 65,892,238–66,502,988; 12q14.3) (illustrated for case 3, Fig. 1B). Using a set of probes spanning *HMGA2* (Table 2) in cases 1–10, we showed that the breakpoints were located

within *HMGA2* in all cases except case 9 (Fig. 2A). In case 9, the breakpoint was centromeric to the 5'UTR of *HMGA2* (Fig. 2A). Case 13 showed a deletion of the region delineated by the RP11-30I11 and RP11-118B13 probes (Supporting Information Fig. S1) whereas in cases 14 and 15 we did not detect any rearrangement of *HMGA2* using these probes.

In case 16, we observed a breakpoint in the interval between RP11-754H10/RP11-661K21 and CTD-2527O17/CTD-2342D14 probes that flank *HMGA1*, indicating a structural rearrangement of *HMGA1* (Fig. 1E).

The 1p32 region contains two genes that we initially considered as candidates: *JUN* in 1p32.1 [amplified in dedifferentiated liposarcomas (DDLPS) (Mariani et al., 2007)], and *ACOT11* in 1p32.3 (involved in mammalian fatty acid metabolism (Kirkby et al., 2010)). We observed that the breakpoints in 1p32 were located neither in *JUN* nor in *ACOT11*. They were located in a telomeric position with regard to *JUN*, and in a centromeric position with regard to *ACOT11* within a 1.5 Mb region delineated by the RP11-485A11 (chr1:

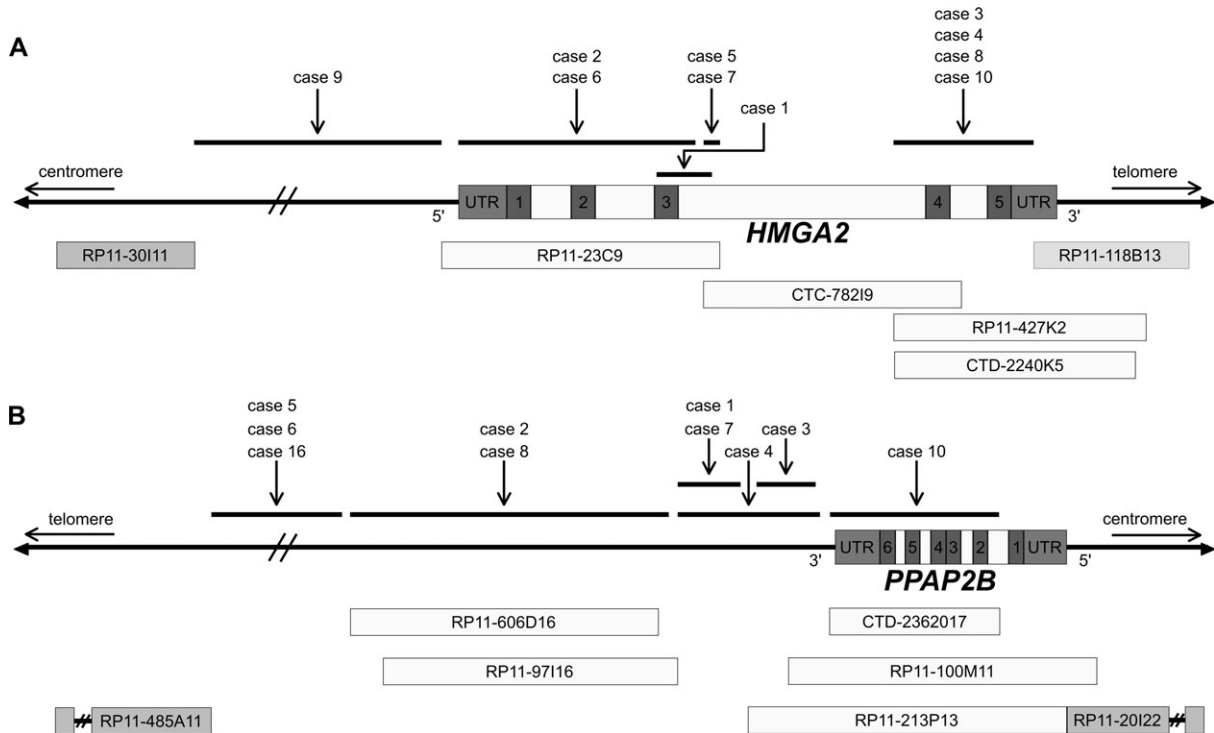


Figure 2. Schematic illustration of the location of the breakpoints on 12q14.3 (A) and 1p32.2 (B) identified by FISH analysis using a series of BAC probes. Horizontal lines delineate the regions of the breakpoints as determined by FISH analysis using the BAC probes mentioned on the scheme. A: Characterization of the 12q14.3 breakpoints in 10 cases of lipomas with t(1;12)(p32.2;q14.3) (cases 1–10).

B: Characterization of the breakpoints on 1p32.2 in nine cases of lipomas with t(1;12)(p32.2;q14.3) (cases 1–8 and 10) and one case of lipoma with t(1;6)(p32.2;p21) (case 16). Case 9 presented a deletion of the region delineated by the RP11-606D16 and RP11-100M11 probes and is therefore not represented on the scheme.

55,708,546–55,908,106; 1p32.3) and RP11-20I22 (chr1: 57,050,331–57,210,976; 1p32.2) BAC probes (illustrated by a split signal of these probes for case 3 in Fig. 1C and case 16 in Fig. 1F). We narrowed down the breakpoints more precisely in cases 1–10 and case 16 (Fig. 2B). According to the genome map, a single gene in this region was correctly oriented to potentially produce a fusion transcript with *HMG2*: *PPAP2B* (Phosphatidic Acid Phosphatase type 2B). In cases 1–10 and case 16, the breakpoints were spread out in a region of approximately 1.3 Mb flanked by BAC probes RP11-485A11 and CTD-2362O17 (Fig. 2B). This region was telomeric of *PPAP2B* 3'UTR. In case 10, we observed a split signal on der(12) and der(1) using CTD-2362O17 BAC probe that spans *PPAP2B* (Fig. 3B) suggesting that this case might present a fusion of *HMG2* with *PPAP2B*.

RT-PCR and Sequencing Analysis of *HMG2*-*PPAP2B* Transcript in Case 10

The sequencing of the RT-PCR product obtained using a forward primer for *HMG2* in

exon 2 and a reverse primer for *PPAP2B* in exon 6 showed an in-frame fusion of the 3'UTR of *HMG2* with exon 6 of *PPAP2B* (Figs. 3D and 3E).

Q-RT-PCR Analysis of *HMG2* and *PPAP2B* Expression

Q-RT-PCR was done for cases 1, 2, 4, 5, 8, 11, and 12 frozen samples of which were available. We observed a strong overexpression of *HMG2* mRNA compared to NSAT in seven of seven cases that always included expression of exons 1 and 2 (Fig. 4A). The fold changes ranged from 231 (case 4) to 4749 (case 11). Exons 3 and 4 were overexpressed in three of seven cases (43%) whereas exon 5 was overexpressed in only two cases (29%). For *PPAP2B* mRNA expression analysis, probes for exons 1–2 and exons 4–5 gave roughly similar results. In contrast to the consistent overexpression of *HMG2* in all cases, *PPAP2B* expression was variable: cases 1, 2 and 5 showed a slight overexpression, cases 4 and 8 showed a decreased expression, and no variation

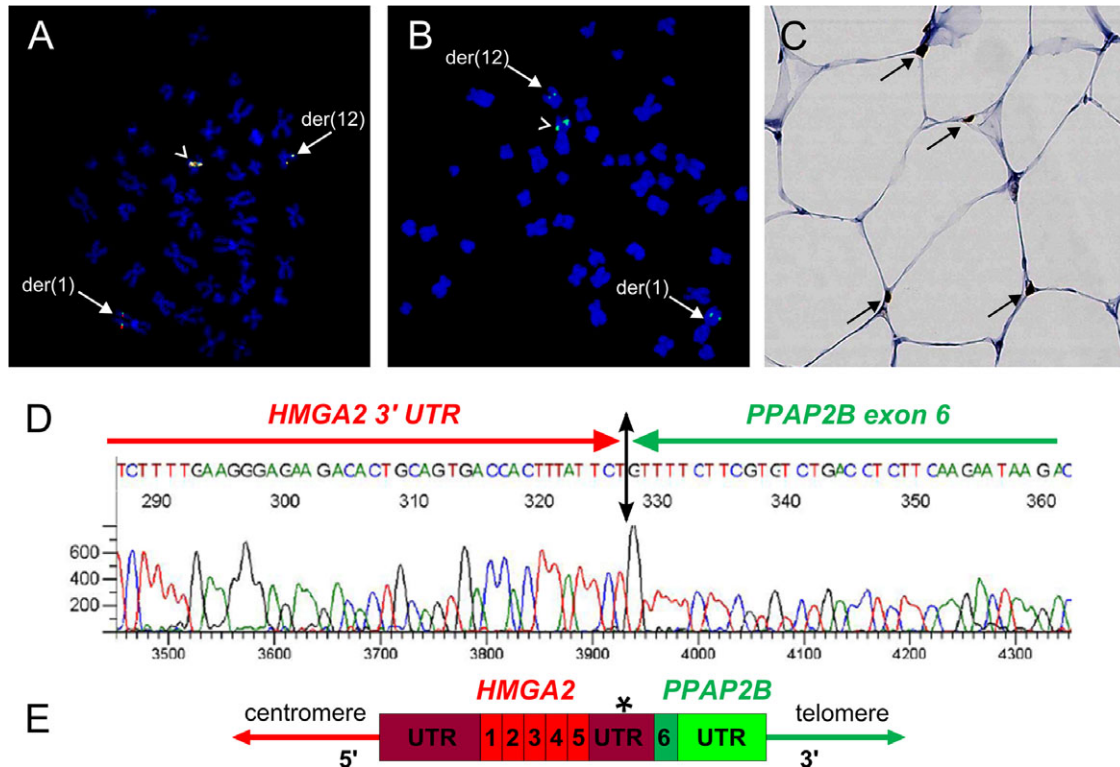


Figure 3. A-B: FISH analysis of *HMGA2* (A) and *PPAP2B* (B) in case 10 using CTD-2240K5 (red signal) and RP11-427K2 (green signal) probes that span the same region of *HMGA2* exons 4 and 5 and 3'UTR (A) and CTD-2362O17 (green signal) that spans the *PPAP2B* gene (B). Fission of *HMGA2* (A) is demonstrated by split red and green signals on der (12) and der (1) (arrows). Fission of *PPAP2B* (B) is demonstrated by split green signals on der (12) and der (1) (arrows). The normal alleles are indicated by arrow-

heads. C: analysis of the *HMGA2* protein by IHC on a representative section of case 10. The arrows indicate a nuclear staining of the *HMGA2* protein. D: chromatogram showing the in-frame fusion of *HMGA2* (3'UTR) with *PPAP2B* (last exon) mRNA in case 10. E: scheme representing the *HMGA2-PPAP2B* fusion transcript resulting from the $t(1;12)(p32;q14.3)$ in case 10. Asterisk indicates a stop codon. [Color figure can be viewed in the online issue, which is available at wileyonlinelibrary.com.]

of expression was detected in cases 11 and 12 (Fig. 4B).

Expression of *HMGA2* Detected by IHC

We showed that *HMGA2* rearrangement in case 10 led to expression of *HMGA2* protein (Fig. 3C). We also detected *HMGA2* protein expression in all $t(1;12)$ cases analyzed (cases 1 to 15) including case 13 showing a deletion of the *HMGA2* region (Supporting Information Fig. S1) and the two cases without *HMGA2* rearrangement (cases 14 and 15) (data not shown).

FISH Analysis of the Ip32.2 Region in a Series of WDLPS/DDLPS

We have analyzed by FISH 10 cases of WDLPS/DDLPS presenting an amplification of *MDM2* including seven cases showing a co-amplification of *JUN*. None of these cases showed an amplification of *PPAP2B* (using the RP11-1089D11 probe) (data not shown), indicating that

PPAP2B does not belong to the *JUN* amplicon in WDLPS/DDLPS.

PPAP2B Expression in hMADS Cells

PPAP2B codes for a lipid phosphate phosphatase. We therefore assumed that it might play a role in human adipogenesis. To test this hypothesis, we used the hMADS cells as a model for adipocyte differentiation. As shown in Figure 5, the expression of *PPAP2B* was significantly downregulated during adipogenic differentiation. The effect was detected late during adipocyte differentiation since *PPAP2B* expression was inhibited 7 days after treatment of hMADS cells with the adipogenic cocktail.

DISCUSSION

Translocation $t(1;12)(p32;q14)$ has been previously reported in lipomas (Mitelman et al., 2012) but it had not been explored at the molecular level. In our series of karyotyped lipomas, this rearrangement appeared to be the second most

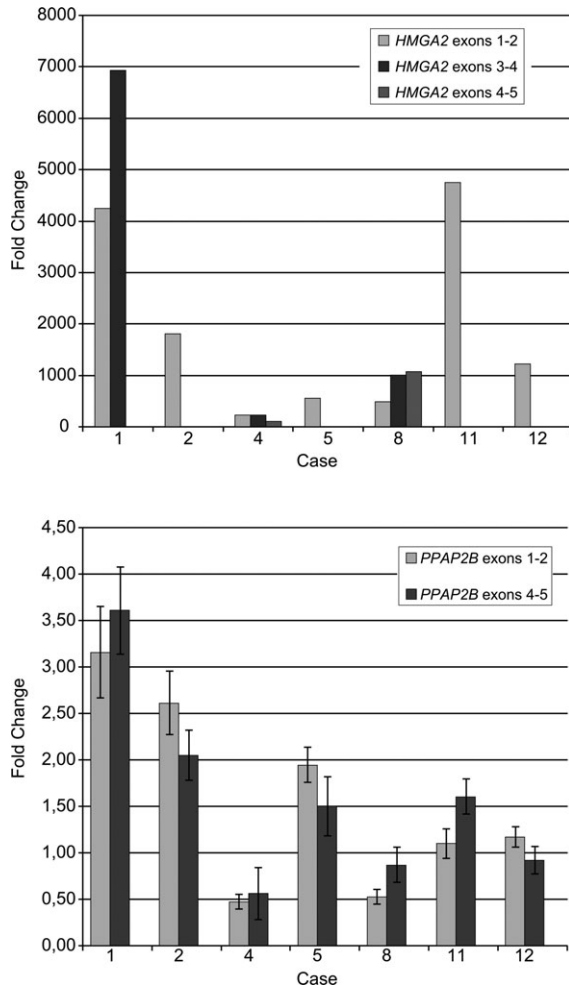


Figure 4. Expression patterns of exons 1–2, exons 3–4, and exons 4–5 of *HMGGA2* (A) and exons 1–2 and exons 4–5 of *PPAP2B* (B) using qRT-PCR in seven lipomas with t(1;12)(p32;q14.3). *HMGGA2* and *PPAP2B* mRNA were expressed as fold changes relative to expression in NSAT from control individuals. Data for *HMGGA2* expression are from an experiment representative of three independent experiments. Data for *PPAP2B* expression are presented as means \pm S. E. of three independent experiments.

frequent after that of t(3;12). We evaluated the frequency of this translocation to be approximately 4% of lipomas with abnormal karyotypes.

We have demonstrated that *PPAP2B* is the translocation partner of *HMGGA2* in lipomas harboring this recurrent t(1;12) translocation. *PPAP2B*, also called *LPP3* for *Lipid Phosphate Phosphatase 3* (the acronym's similarity to *LPP-Lipoma Preferred Partner* is fortuitous), belongs to the lipid phosphate phosphatases family which comprises three members: *LPP1*, *LPP2* and *LPP3*. *PPAP2B* codes for a membrane glycoprotein containing six transmembrane domains widely expressed in human tissues (Sigal et al., 2005) that hydrolyses lipid phosphates including lysophosphatidic acid (LPA) and sphingosine

1-phosphate. Invalidation of the murine *Ppap2b* gene results in embryonic lethality due to defects in both vasculogenesis and patterning during early development (Escalante-Alcalde et al., 2003). *PPAP2B* was also reported to play a critical role in neuron differentiation and neurite outgrowth (Sanchez-Sanchez et al., 2012). LPA and sphingosine 1-phosphate are bioactive lipids that can induce proliferation, survival, and invasiveness in certain cell types and *PPAP2B* might exert an anti-tumorigenic effect by limiting LPA signalling. Overexpression of *PPAP2B* has been shown to decrease growth, survival, and tumorigenesis of ovarian cancer cells (Tanyi et al., 2003). A limited number of studies have reported the potential involvement of *PPAP2B* in tumorigenesis: *PPAP2B* has been identified as a Myc-bound locus in medulloblastoma cells (Zhou et al., 2010) and shown to regulate tumor growth via β -catenin and cyclin D1 signaling in glioblastoma (Chatterjee et al., 2011).

We have shown that in nine out of 10 t(1;12) cases and one t(1;6) case, the breakpoints were located in 3' extragenic region flanking *PPAP2B* 3'UTR, in a distance range of 100–800 kb. Case 10 was the only one presenting a breakpoint within the *PPAP2B* gene resulting in fusion of the last exon of *PPAP2B* (exon 6) with the *HMGGA2* 3'UTR. The potential consequences of extragenic breakpoints in the alteration of expression of *PPAP2B* are not known. Data reporting expression of *PPAP2B* in adult human tissues are scarce. *PPAP2B* mRNA appear widely distributed (Kai et al., 1997; Humtsoe et al., 2003; Sigal et al., 2005). Expression profiles based on detection of EST (expressed sequence tag) transcripts

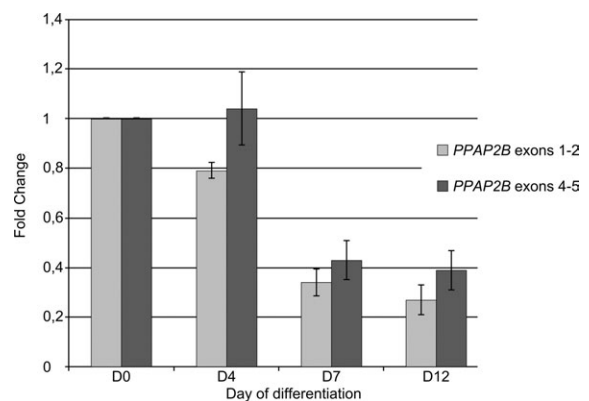


Figure 5. Expression pattern of exons 1–2 and exons 4–5 of *PPAP2B* using qRT-PCR during adipocyte-differentiation of hMADS cells. *PPAP2B* mRNA was expressed as fold changes relative to expression in undifferentiated hMADS cells (Day 0: D0). Data are presented as means \pm S.E. of three independent experiments.

in human adult tissues show heterogeneous levels of expression: in particular, vascular system, placenta, prostate, lymph node, and mammary gland express high levels of *PPAP2B* whereas skin, spleen and thymus show no expression (Sigal et al., 2005). In the absence of currently available reliable antibodies for IHC studies, we explored the expression of *PPAP2B* mRNA in NSAT and lipomas using qRT-PCR. We found that *PPAP2B* mRNA was quite abundant in NSAT. The expression levels in t(1;12) lipomas were also significant but variable. They were apparently not correlated to the presence or absence of the t(1;12) translocation. Therefore these data need to be extended to additional cases. It can be hypothesized that only a slight alteration of *PPAP2B* expression levels, sufficient for giving a selective advantage to tumor cells but difficult to detect, might result from the genomic rearrangement. It can also be hypothesized that the rearrangement does not impact *PPAP2B* expression but only affects *HMGA2*. Indeed, some studies suggest that the critical event leading to *HMGA2* oncogenicity relies on its truncation, regardless of the nature of the fused sequences (Fedele et al., 1998; Arlotta et al., 2000). However, an intrinsic role for fusion partners has also been suggested. For instance, the *HMGA2-LPP* fusion transcript always contains at least the last three exons of *LPP* leading to the expression of either two or three LIM domains of the LPP protein, domains that have a function in cell migration, proliferation and transcription [reviewed in (Grunewald et al., 2009)]. Moreover, Kubo et al. (2009) have reported three cases of lipomas with t(3;12) for which the only transcript they could detect using RT-PCR was the reciprocal *LPP-HMGA2* transcript suggesting a role for *LPP* in the tumorigenesis of these lipomas.

The location of the *HMGA2* breakpoints in our t(1;12) series was variable. It was intragenic for all cases except in case 9 that showed an extragenic 5' breakpoint (Fig. 2). In case 10, we have found that the rearrangement fuses the 3'UTR region of *HMGA2* with exon 6 of *PPAP2B*. Breakpoints occurring in the 3'UTR of *HMGA2* have been previously described in three cases of lipomas (Schoenmakers et al., 1995; Wang et al., 2009) as well as in other types of tumors, such as leiomyomas (Quade et al., 2003), pleomorphic adenomas (Geurts et al., 1997), polycythemia vera (Storlazzi et al., 2006) and paroxysmal nocturnal hemoglobinuria (Inoue et al., 2006). Interestingly, the breakpoint that we have identified in case 10

(80 bp downstream of the stop codon) is very close to the breakpoints reported in two lipomas described by Wang et al. (2009) which were 97 and 106 bp downstream to the stop codon, respectively. Moreover, Medeiros et al. (2007) have reported a breakpoint occurring in *HMGA2* at the same position as in case 10 in a case of aggressive angiomyxoma presenting a t(1;12) (p32;q14). The authors have located the breakpoint in the 1p32 region 496 bp downstream from the *PPAP2B* 3'UTR. This indicates that *PPAP2B* rearrangements might be involved in tumors other than lipomas. We showed a strong overexpression of *HMGA2* mRNA (at least exons 1 and 2) and protein in all t(1;12) cases, including case 13 that harbored a deletion of the *HMGA2* region and cases 14 and 15 without detectable rearrangement of this region (Table 1). In case 10, we can predict from the sequencing of the fusion transcript an expression of the full length *HMGA2* protein. Note that the breakpoint in the *HMGA2* 3'UTR was located downstream from the first *let-7* microRNA (miRNA) binding site. The 3'UTR of *HMGA2* indeed contains multiple binding sites for the *let-7* family. Targeted mutations of these binding sites or functional inactivation of *let-7* result in upregulation of *HMGA2* (Lee and Dutta, 2007; Mayr et al., 2007). Our results confirm that deletion of the *let-7* binding sites results in *HMGA2* overexpression. They also demonstrate that elimination of the first *let-7* binding site is not critical for upregulation of *HMGA2* as reported by Wang et al. (2009).

Interestingly, *PPAP2B* also appears to be a translocation partner for *HMGA1* in a t(1;6)(p32;p21) case suggesting that *HMGA1* might play a role similar to that of *HMGA2* in t(1;6) lipomas.

We have demonstrated previously that *NFIB* is a recurrent fusion partner of *HMGA2* in lipomas (Italiano et al., 2008b). *NFIB* is involved in the pathogenesis of benign tumors but also in malignant tumors such as the adenoid cystic carcinomas of the breast and salivary glands (Marchio et al., 2010). Interestingly, besides its role in tumorigenesis, *NFIB* has recently been shown to play a role in adipocyte differentiation (Waki et al., 2011). Our hypothesis was that it might also be the case for *PPAP2B*. To test this hypothesis, we used the hMADS cells as a model for adipocyte differentiation. These cells exhibit the characteristics of mesenchymal stem cells and they can in vitro differentiate into cells that display a unique combination of properties similar, if not identical, to those of native human

adipocytes (Bezaire et al., 2009; Poitou et al., 2009). Our results showed that differentiation of hMADS cells in adipocytes was associated with a strong down regulation of *PPAP2B* expression suggesting that *PPAP2B* might play a role in human adipogenesis. Our results validate in a human model the results obtained on the mouse preadipocyte cell line 3T3F442A (Simon et al., 2002). The involvement of *PPAP2B* in adipogenesis might occur through the control of LPA production. Indeed, Simon et al. (2002) have shown that down regulation of *PPAP2B* during differentiation of 3T3F442A preadipocytes into adipocytes is concomitant to and might be responsible for a strong reduction in LPA phosphatase activity resulting in an increased production of LPA by the adipocytes.

ACKNOWLEDGMENTS

The authors are grateful to J.M. Coindre (Institut Bergonié, Bordeaux) for providing lipoma samples and histological data. They thank F. Keslair and R. Grattery for skilful technical assistance.

REFERENCES

- Arlotta P, Tai AK, Manfioletti G, Clifford C, Jay G, Ono SJ. 2000. Transgenic mice expressing a truncated form of the high mobility group I-C protein develop adiposity and an abnormally high prevalence of lipomas. *J Biol Chem* 275:14394–14400.
- Ashar HR, Fejzo MS, Tkachenko A, Zhou X, Fletcher JA, Wercmowicz S, Morton CC, Chada K. 1995. Disruption of the architectural factor HMG1-C: DNA-binding AT hook motifs fused in lipomas to distinct transcriptional regulatory domains. *Cell* 82:57–65.
- Bartuma H, Hallor KH, Panagopoulos I, Collin A, Rydholm A, Gustafson P, Bauer HC, Brosjö O, Domanski HA, Mandahl N, Mertens F. 2007. Assessment of the clinical and molecular impact of different cytogenetic subgroups in a series of 272 lipomas with abnormal karyotype. *Genes Chromosomes Cancer* 46:594–606.
- Bezaire V, Mairal A, Ribet C, Lefort C, Grousse A, Jocken J, Laurencikienė J, Anesia R, Rodriguez AM, Ryden M, Stenson BM, Dani C, Ailhaud G, Arner P, Langin D. 2009. Contribution of adipose triglyceride lipase and hormone-sensitive lipase to lipolysis in hMADS adipocytes. *J Biol Chem* 284:18282–18291.
- Bianchini L, Saada E, Gjernes E, Marty M, Haudebourg J, Birtwisle-Peyrottes I, Keslair F, Chignon-Sicard B, Chamorey E, Pedeutour F. 2011. Let-7 microRNA and HMG2 levels of expression are not inversely linked in adipocytic tumors: Analysis of 56 lipomas and liposarcomas with molecular cytogenetic data. *Genes Chromosomes Cancer* 50:442–455.
- Broberg K, Zhang M, Strombeck B, Isaksson M, Nilsson M, Mertens F, Mandahl N, Panagopoulos I. 2002. Fusion of RDC1 with HMG2 in lipomas as the result of chromosome aberrations. *Int J Oncol* 21:321–326.
- Chatterjee I, Humtsoe JO, Kohler EE, Sorio C, Wary KK. 2011. Lipid phosphate phosphatase-3 regulates tumor growth via beta-catenin and cyclin D1 signaling. *Mol Cancer* 10:51.
- Choi YW, Choi JS, Zheng LT, Lim YJ, Yoon HK, Kim YH, Wang YP, Lim Y. 2007. Comparative genomic hybridization array analysis and real time PCR reveals genomic alterations in squamous cell carcinomas of the lung. *Lung Cancer* 55:43–51.
- Dahlén A, Mertens F, Rydholm A, Brosjö O, Wejde J, Mandahl N, panagopoulos I. 2003. Fusion, disruption, and expression of HMG2 in bone and soft tissue chondromas. *Mod Pathol* 16:1132–1140.
- Dooley AL, Winslow MM, Chiang DY, Banerji S, Stransky N, Dayton TL, Snyder EL, Senna S, Whittaker CA, Bronson RT, Crowley D, Barretina J, Garraway L, Meyerson M, Jacks T. 2011. Nuclear factor I/B is an oncogene in small cell lung cancer. *Genes Dev* 25:1470–1475.
- Escalante-Alcalde D, Hernandez L, Le Stunff H, Maeda R, Lee HS, Jr Gang C, Sciorra VA, Daar I, Spiegel S, Morris AJ, Stewart CL. 2003. The lipid phosphatase LPP3 regulates extra-embryonic vasculogenesis and axis patterning. *Development* 130:4623–4637.
- Fedele M, Berlingieri MT, Scala S, Chiariotti L, Viglietto G, Rippe V, Bullerdick J, Santoro M, Fusco A. 1998. Truncated and chimeric HMG1-C genes induce neoplastic transformation of NIH3T3 murine fibroblasts. *Oncogene* 17:413–418.
- Fletcher CDM, Unni KK, Mertens F, editors. 2002. World Health Organization Classification of Tumours. Pathology and Genetics of Tumours of Soft Tissue and Bone. Lyon: IARC Press
- Gabriellsson BG, Olofsson LE, Sjogren A, Jernas M, Elander A, Lonn M, Rudemo M, Carlsson LM. 2005. Evaluation of reference genes for studies of gene expression in human adipose tissue. *Obes Res* 13:649–652.
- Geurts JM, Schoenmakers EF, Van de Ven WJ. 1997. Molecular characterization of a complex chromosomal rearrangement in a pleomorphic salivary gland adenoma involving the 3'-UTR of HMGIC. *Cancer Genet Cytogenet* 95:198–205.
- Geurts JM, Schoenmakers EF, Roijer E, Astrom AK, Stenman G, van de Ven WJ. 1998. Identification of NFIB as recurrent translocation partner gene of HMGIC in pleomorphic adenomas. *Oncogene* 16:865–872.
- Grunewald TGP, Pasdag SM, Butt E. 2009. Cell Adhesion and Transcriptional Activity - Defining the Role of the Novel Proto-oncogene LPP. *Transl Oncol* 2:107–116.
- Han W, Jung EM, Cho J, Lee JW, Hwang KT, Yang SJ, Kang JJ, Bae JY, Jeon YK, Park IA, Nicolau M, Jeffrey SS, Noh DY. 2008. DNA copy number alterations and expression of relevant genes in triple-negative breast cancer. *Genes Chromosomes Cancer* 47:490–499.
- Hatano H, Morita T, Ogose A, Hotta T, Kobayashi H, Segawa H, Uchiyama T, Takenouchi T, Sato T. 2008. Clinicopathological features of lipomas with gene fusions involving HMG2. *Anticancer Res* 28:535–538.
- Humtsoe JO, Feng S, Thakker GD, Yang J, Hong J, Wary KK. 2003. Regulation of cell-cell interactions by phosphatidic acid phosphatase 2b/VCIP. *EMBO J* 22:1539–1554.
- Hussenet T, Mallem N, Redon R, Jost B, Aurias A, du Manoir S. 2006. Overlapping 3q28 amplifications in the COMA cell line and undifferentiated primary sarcoma. *Cancer Genet Cytogenet* 169:102–113.
- Inoue N, Izui-Sarumaru T, Murakami Y, Endo Y, Nishimura J, Kurokawa K, Kuwayama M, Shime H, Machii T, Kanakura Y, Meyers G, Wittwer C, Chen Z, Babcock W, Frei-Lahr D, Parker CJ, Kinoshita T. 2006. Molecular basis of clonal expansion of hematopoiesis in 2 patients with paroxysmal nocturnal hemoglobinuria (PNH). *Blood* 108:4232–4236.
- Italiano A, Bianchini L, Keslair F, Bonnafoos S, Cardot-Leccia N, Coindre JM, Dumollard JM, Hofman P, Leroux A, Mainguene C, Peyrottes I, Ranchere-Vince D, Terrier P, Tran A, Gual P, Pedeutour F. 2008a. HMG2 is the partner of MDM2 in well-differentiated and dedifferentiated liposarcomas whereas CDK4 belongs to a distinct inconsistent amplicon. *Int J Cancer* 122:2233–2241.
- Italiano A, Ebran N, Attias R, Chevallier A, Monticelli I, Mainguene C, Benchimol D, Pedeutour F. 2008b. NFIB rearrangement in superficial, retroperitoneal, and colonic lipomas with aberrations involving chromosome band 9p22. *Genes Chromosomes Cancer* 47:971–977.
- Kai M, Wada I, Imai S, Sakane F, Kanoh H. 1997. Cloning and characterization of two human isozymes of Mg²⁺-independent phosphatidic acid phosphatase. *J Biol Chem* 272:24572–24578.
- Kirkby B, Roman N, Kobe B, Kellie S, Forwood JK. 2010. Functional and structural properties of mammalian acyl-coenzyme A thioesterases. *Prog Lipid Res* 49:366–377.
- Kubo T, Matsui Y, Naka N, Araki N, Goto T, Yukata K, Endo K, Yasui N, Myoui A, Kawabata H, Yoshikawa H, Ueda T. 2009. Expression of HMG2-LPP and LPP-HMG2 fusion genes in lipoma: Identification of a novel type of LPP-HMG2 transcript in four cases. *Anticancer Res* 29:2357–2360.

- Lee YS, Dutta A. 2007. The tumor suppressor microRNA let-7 represses the HMGA2 oncogene. *Genes Dev* 21:1025–1030.
- Mandahl N, Hoglund M, Mertens F, Rydholm A, Willen H, Brosjö O, Mitelman F. 1994. Cytogenetic aberrations in 188 benign and borderline adipose tissue tumors. *Genes Chromosomes Cancer* 9:207–215.
- Marchio C, Weigelt B, Reis-Filho JS. 2010. Adenoid cystic carcinomas of the breast and salivary glands (or ‘The strange case of Dr Jekyll and Mr Hyde of exocrine glands carcinomas). *J Clin Pathol* 63:220–228.
- Mariani O, Brennetot C, Coindre JM, Gruel N, Ganem C, Delattre O, Stern MH, Aurias A. 2007. JUN oncogene amplification and overexpression block adipocytic differentiation in highly aggressive sarcomas. *Cancer Cell* 11:361–374.
- Mayr C, Hemann MT, Bartel DP. 2007. Disrupting the pairing between let-7 and Hmga2 enhances oncogenic transformation. *Science* 315:1576–1579.
- Medeiros F, Erickson-Johnson MR, Keeney GL, Clayton AC, Nascimento AG, Wang X, Oliveira AM. 2007. Frequency and characterization of HMGA2 and HMGA1 rearrangements in mesenchymal tumors of the lower genital tract. *Genes Chromosomes Cancer* 46:981–990.
- Mitelman F, Johansson B, Mertens F, editors. 2012. Mitelman Database of Chromosome Aberrations and Gene Fusions in Cancer. Available at: <http://cgap.nci.nih.gov/Chromosomes/Mitelman>. Accessed October 20, 2012.
- Nilsson M, Panagopoulos I, Mertens F, Mandahl N. 2005. Fusion of the HMGA2 and NFIB genes in lipoma. *Virchows Arch* 447:855–858.
- Nilsson M, Mertens F, Hoglund M, Mandahl N, Panagopoulos I. 2006. Truncation and fusion of HMGA2 in lipomas with rearrangements of 5q32–>q33 and 12q14–>q15. *Cytogenet Genome Res* 112:60–66.
- Nishio J. 2011. Contributions of cytogenetics and molecular cytogenetics to the diagnosis of adipocytic tumors. *J Biomed Biotechnol* 2011:524067.
- Petit MM, Mols R, Schoenmakers EF, Mandahl N, Van de Ven WJ. 1996. LPP, the preferred fusion partner gene of HMGIC in lipomas, is a novel member of the LIM protein gene family. *Genomics* 36:118–129.
- Petit MM, Schoenmakers EF, Huysmans C, Geurts JM, Mandahl N, Van de Ven WJ. 1999. LHFP, a novel translocation partner gene of HMGIC in a lipoma, is a member of a new family of LHFP-like genes. *Genomics* 57:438–441.
- Pierron A, Fernandez C, Saada E, Keslair F, Hery G, Zattara H, Pedetour F. 2009. HMGA2-NFIB fusion in a pediatric intramuscular lipoma: A novel case of NFIB alteration in a large deep-seated adipocytic tumor. *Cancer Genet Cytogenet* 195:66–70.
- Poitou C, Divoux A, Faty A, Tordjman J, Hugol D, Aissat A, Keophipath M, Henegar C, Commans S, Clement K. 2009. Role of serum amyloid A in adipocyte-macrophage cross talk and adipocyte cholesterol efflux. *J Clin Endocrinol Metab* 94:1810–1817.
- Quade BJ, Weremowicz S, Neskey DM, Vanni R, Ladd C, Dal Cin P, Morton CC. 2003. Fusion transcripts involving HMGA2 are not a common molecular mechanism in uterine leiomyomata with rearrangements in 12q15. *Cancer Res* 63:1351–1358.
- Rodriguez AM, Pisani D, Dechesne CA, Turc-Carel C, Kurzenne JY, Wdzickowski B, Villageois A, Bagnis C, Breittmayer JP, Groux H, Ailhaud G, Dani C. 2005. Transplantation of a multipotent cell population from human adipose tissue induces dystrophin expression in the immunocompetent mdx mouse. *J Exp Med* 201:1397–13405.
- Rogalla P, Kazmierczak B, Meyer-Bolte K, Tran KH, Bullerdiek J. 1998. The t(3;12)(q27;q14–q15) with underlying HMGIC-LPP fusion is not determining an adipocytic phenotype. *Genes Chromosomes Cancer* 22:100–104.
- Sanchez-Sanchez R, Morales-Lazaro SL, Baizabal JM, Sunkara M, Morris AJ, Escalante-Alcalde D. 2012. Lack of lipid phosphate phosphatase-3 in embryonic stem cells compromises neuronal differentiation and neurite outgrowth. *Dev Dyn* 241:953–964.
- Schoenmakers EF, Wanschura S, Mols R, Bullerdiek J, Van den Bergh H, Van de Ven WJ. 1995. Recurrent rearrangements in the high mobility group protein gene, HMGI-C, in benign mesenchymal tumours. *Nat Genet* 10:436–444.
- Sigal YJ, McDermott MI, Morris AJ. 2005. Integral membrane lipid phosphatases/phosphotransferases: Common structure and diverse functions. *Biochem J* 387:281–293.
- Simon MF, Rey A, Castan-Laurel I, Gres S, Sibrac D, Valet P, Saulnier-Blache JS. 2002. Expression of ectolipid phosphate phosphohydrolases in 3T3F442A preadipocytes and adipocytes. Involvement in the control of lysophosphatidic acid production. *J Biol Chem* 277:23131–23136.
- Storlazzi CT, Albano F, Locunolo C, Lonoce A, Funes S, Guastadisegni MC, Cimarosto L, Impera L, D’Addabbo P, Panagopoulos I, Specchia G, Rocchi M. 2006. t(3;12)(q26;q14) in polycythemia vera is associated with upregulation of the HMGA2 gene. *Leukemia* 20:2190–2192.
- Tanyi JL, Morris AJ, Wolf JK, Fang X, Hasegawa Y, Lapushin R, Auersperg N, Sigal YJ, Newman RA, Felix EA, Atkinson EN, Mills GB. 2003. The human lipid phosphate phosphatase-3 decreases the growth, survival, and tumorigenesis of ovarian cancer cells: Validation of the lysophosphatidic acid signaling cascade as a target for therapy in ovarian cancer. *Cancer Res* 63:1073–1082.
- Waki H, Nakamura M, Yamauchi T, Wakabayashi K, Yu J, Hirose-Yotsuya L, Take K, Sun W, Iwabu M, Okada-Iwabu M, Fujita T, Aoyama T, Tsutsumi S, Ueki K, Kodama T, Sakai J, Aburatani H, Kadowaki T. 2011. Global mapping of cell type-specific open chromatin by FAIRE-seq reveals the regulatory role of the NFI family in adipocyte differentiation. *PLoS Genet* 7:e1002311.
- Wang X, Hulshizer RL, Erickson-Johnson MR, Flynn HC, Jenkins RB, Lloyd RV, Oliveira AM. 2009. Identification of novel HMGA2 fusion sequences in lipoma: Evidence that deletion of let-7 miRNA consensus binding site 1 in the HMGA2 3’ UTR is not critical for HMGA2 transcriptional upregulation. *Genes Chromosomes Cancer* 48:673–678.
- Zaragosi LE, Ailhaud G, Dani C. 2006. Autocrine fibroblast growth factor 2 signaling is critical for self-renewal of human multipotent adipose-derived stem cells. *Stem Cells* 24:2412–2419.
- Zhou L, Picard D, Ra YS, Li M, Northcott PA, Hu Y, Stearns D, Hawkins C, Taylor MD, Rutka J, Der SD, Huang A. 2010. Silencing of thrombospondin-1 is critical for myc-induced metastatic phenotypes. *Cancer Res* 70:8199–8210.
- Zhou Z, Flesken-Nikitin A, Corney DC, Wang W, Goodrich DW, Roy-Burman P, Nikitin AY. 2006. Synergy of p53 and Rb deficiency in a conditional mouse model for metastatic prostate cancer. *Cancer Res* 66:7889–7898.